Hydration Effects of Heparin on Antithrombin Probed by Osmotic Stress

Maria P. McGee,* Jie Liang,† and James Luba*
*Wake Forest University Medical School, Medicine and Biochemistry Departments, Medical Center Boulevard, Winston-Salem, North Carolina 27157 USA; and †University of Illinois at Chicago, Bioengineering Department, Chicago, Illinois 60607 USA

ABSTRACT Antithrombin is a key inhibitor of blood coagulation proteases and a prototype metastable protein. Heparin binding to antithrombin induces conformational transitions distal to the binding site. We applied osmotic stress techniques and rate measurements in the stopped flow fluorometer to investigate the possibility that hydration changes are associated with these transitions. Water transfer was identified from changes in the free energy of activation, $\Delta G‡$, with osmotic pressure π. The $\Delta G‡$ was determined from the rate of fluorescence enhancement/decrease associated with heparin binding/release. The volume of water transferred, ΔV, was determined from the relationship, $\Delta G/\pi = \Delta V$. With an osmotic probe of 4 Å radius, the volumes transferred correspond to 158 ± 11 water molecules from reactants to bulk during association and 162 ± 22 from bulk to reactants during dissociation. Analytical characterization of water-permeable volumes in x-ray-derived bound and free antithrombin structures were correlated with the volumes measured in solution. Volume changes in water permeable pockets were identified at the loop-insertion and heparin-binding regions. Analyses of the pockets' atomic composition indicate that residues Ser-79, Ala-86, Val-214, Leu-215, Asn-217, Ile-219, and Thr-218 contribute atoms to both the heparin-binding pockets and to the loop-insertion region. These results demonstrate that the increases and decreases in the intrinsic fluorescence of antithrombin during heparin binding and release are linked to dehydration and hydration reactions, respectively. Together with the structural analyses, results also suggest a direct mechanism linking heparin binding/release to loop expulsion/insertion.

INTRODUCTION

Antithrombin is a circulating serine proteinase inhibitor essential for the control of blood coagulation reactions (Jordan et al., 1980; Olson et al., 1993). Congenital or acquired antithrombin deficiencies are associated with thrombosis (Lane et al., 1992; Beauchamp et al., 1998). Antithrombin's inhibitory activity is potentiated by the sulfated glycosaminoglycan heparin, which induces conformational changes that increase antithrombin's binding affinity for its target proteinases by several orders of magnitude. These conformational changes are associated with spectral changes including an enhancement of ~40% in intrinsic protein fluorescence (Olson and Shore, 1981; Huntington et al., 1996). Subsequent interaction of the heparin/antithrombin complex with the proteinase is linked to both reversal of the fluorescence enhancement and release of the heparin (Craig et al., 1989).

The activating conformational changes propagate throughout the antithrombin structure in ways that are not completely understood but that appear to involve allosteric mechanisms (Lawrence, 1997; Wilczynska et al., 1997; Gils and Declerk, 1998). The transition from the circulating native conformation to the activated, heparin-bound, antithrombin conformation includes the release of the reactive center loop from an inserted position between two strands of a β-sheet structure in the protein's core. In x-ray-derived models of unbound native antithrombin, the reactive center loop is partially inserted into the β-sheet (Schereuder et al., 1994; Skinner et al., 1997; Carrell et al., 1991). In the only one available x-ray-derived model of bound, activated antithrombin, the reactive loop is free and completely exposed to solvent. In this structure, the heparin-binding groove (Ersdal-Badju et al., 1998) is partially occupied by an oversulfated heparin analog, pentasaccharide (Jin et al., 1997). It has been proposed that antithrombin circulates in a metastable state that is destabilized by heparin during initial binding. The alteration in the rate and/or sequence of conformational changes at the loop insertion-region observed in certain antithrombin mutants is considered a prototype mechanism of "conformational disease" (Beauchamp et al., 1998; Zou et al., 1999). Kinetically, considerable evidence indicates that the heparin-antithrombin interaction is a two-step reaction with a strong electrostatic component. An initial, low-affinity step equilibrates very rapidly and induces conformational transitions leading to high-affinity interactions (Olson et al., 1993; Desai et al., 1998). The subsequent inhibition of the proteinase is also a two-step process with initial fast equilibration and readily reversible formation of a ternary complex). Interactions in the ternary complex lead via an acyl-enzyme intermediate to heparin release and formation of an irreversible antithrombin-proteinase complex (Kvassman et al., 1998). Recent structure/function analyses also indicate that proteinase inhibition and heparin release are linked to reinsertion of the reactive loop into the β-sheet and translocation of the proteinase from its initial low-affinity interaction site in the exposed reactive loop to the other end of the antithrombin molecule (Stratikos and Gettins, 1999).

Submitted May 10, 2001, and accepted for publication November 15, 2001.

Address reprint requests to: Maria P. McGee, Wake Forest University Medical School, Medicine and Biochemistry Departments, Medical Center Boulevard, Winston-Salem, NC 27157. Tel.: 336-716-6716; Fax: 336-716-9821; E-mail: mmcgee@wfubmc.edu.

0006-3495/02/02/1040/10 $2.00

In this study, we exploit osmotic stress (OS) techniques to examine the conformational transitions and the putative allosteric regulation of antithrombin function by heparin. The technique of OS has been previously used to investigate the role of water in the regulation of hemoglobin oxygenation and other reactions (Colombo et al., 1992; Douzou, 1994; Parsegian et al., 2000; Rand, 1992). The approach is based on the well-established observation that the volume of functional proteins changes with their conformation (Johnson and Eyrin, 1970). In contrast to studies using hydrostatic pressure, OS technique measures the net number of water molecules gained or lost from spaces inaccessible to cosolutes rather than the changes in the hydration density (Hochachka and Somero, 1973). Recent functional studies indicate that osmotic stress induced with several osmolytes influences the binding parameters of the heparin antithrombin reactions. Here, we combine stopped-flow kinetic measurements and OS to analyze net water transfer during the association and dissociation of heparin. The water-transfer measurements in solution are buttressed by structural studies, using analytical geometry (Liang et al., 1998) on x-ray-derived models of antithrombin conformers (Skinner et al., 1997, 1998; Jin et al., 1997). Results indicate that osmotic potentials change the free energy of antithrombin/heparin association/dissociation reactions. Osmotic stress increases the association rate and decreases the dissociation rate, demonstrating concomitant dehydration and hydration reactions, respectively. Analysis of the water-permeable pockets in x-ray-derived structures provides further insight into the hydration effects. Hydration volumes differs among bound and free and loop-inserted and loop-exposed antithrombin models and correlate with data from reaction kinetics in solution.

MATERIALS AND METHODS

Osmotic stress technique

The theoretical basis of the OS technique has been described and validated in detail before (Parsegian et al., 1986; Rand, 1992; Colombo et al., 1992) and revised recently (Parsegian et al., 2000). Briefly, functional reactions of complex proteins like antithrombin are associated with conformational transitions that drastically alter the magnitude and distribution of their water-permeable spaces (Liang and McGee, 1998; Liang et al., 1998). When the reactions proceed in the presence of cosolutes that are excluded from the water-permeable spaces, the difference in osmotic pressure between the excluded spaces and bulk solution generates a potential that contributes to the free energy changes.

In the present studies, we use polyethylene glycol with radius ~4 Å, as an osmotic probe. The rate of reactions that are linked to water transfer from reactants to bulk solution is expected to accelerate, whereas the rate of reactions that are associated with transfer from bulk to reactants is expected to decrease. Similarly, at equilibrium, the probe will decrease the dissociation constant, if excluded spaces in the complex have less water than in the unbound reactants. Net volume of water transfer is determined from the change in free energy with osmotic potential. The osmotic potential between excluded spaces and bulk solution is controlled by increasing the concentration of polyethylene glycol (PEG) in bulk solution. The direction of water transfer is determined from the $\Delta G/\pi$ slope: when the slope is positive, the transfer is from bulk to reactants and in the opposite direction from the osmotic potential; when the slope is negative, transfer is from reactants to bulk and in the same direction as the osmotic potential. Changes in free energy are determined from equilibrium and reaction constants according to thermodynamic principles (Glasstone et al., 1941):

$$\Delta G = -\mathrm{R}T \ln \mathbf{K} \quad (1)$$

$$\Delta G^{\ddagger} = -\mathrm{R}T \ln \mathbf{k}h/\mathrm{k_B}\,T, \quad (2)$$

in which **K** and **k** are equilibrium and rate constants for the complex and reaction rate, respectively, R is the gas constant (1.987 cal/mol/degree); T is the temperature (Kelvin); h is Plank's constant (1.584×10^{-34} cal s^{-1}); and k_B is Boltzmann's constant (3.29×10^{-24} cal/degree). The volume of water transfer is calculated from the equivalence: 1 atm × (volume of 1 mol of water) = 0.435 cal/mol. Thus, from the measured differential ratio $\Delta G/\Delta\pi$, (cal/mol/atm)/0.435 = mol H_2O.

Determination of reaction rates and equilibrium binding parameters

Reaction scheme

The effect of osmotic stress on the association and dissociation rate and on the equilibrium-binding parameters of the antithrombin/heparin interaction was analyzed on the basis of the previously validated (Olson et al., 1993) kinetic scheme:

$$\mathrm{AT} + \mathrm{H} \overset{\mathrm{Kh}}{\Leftrightarrow} \mathrm{AT^*.H} + \mathrm{fXa} \overset{\mathrm{Kt}}{\Leftrightarrow} \mathrm{H.AT^*} - \mathrm{Xa} \overset{\mathrm{k}}{\Rightarrow} \mathrm{AT.fXa} + \mathrm{H} \quad (3)$$

in which Kh is the dissociation constant for the antithrombin/heparin interaction, Kt is the dissociation constant for the ternary interaction between fXa (coagulation factor Xa) and the antithrombin/heparin complex, and k is the first-order rate constant for the stabilization of the inhibitory complex.

The stabilization of the inhibitory complex is closely linked to the release of heparin and the reversal of the conformational changes responsible for the intrinsic fluorescence enhancement. Although it is not clear how reversal of fluorescence intensity is mechanistically linked to the antithrombin/proteinase interactions in the ternary complex, detailed kinetic analyses indicate that dissociation occurs either simultaneously or in a faster, step subsequent to the first-order stabilizing step (Craig et al., 1989). Therefore, the rate of fluorescence decrease can be used to follow the rate of conformational changes linked to heparin dissociation.

Fluorescence enhancement saturation curves

The effect of osmotic stress on the binding parameters of antithrombin and heparin was measured at fixed antithrombin concentrations under equilibrium conditions. Osmotic stress was induced by including polyethylene glycol in the solutions. The fraction of antithrombin complexed with heparin in either control or stressed solutions was determined from the enhancement of tryptophan fluorescence in bound, relative to free, antithrombin. The enhancement in the intrinsic fluorescence of antithrombin after 10 to 13 successive additions of heparin (200–2000 nM) was monitored in a SLM 8000 photon-counting spectrofluorometer (λ_{ex} 280 nm, λ_{em} 340 nm) with both slits at 4 nm. The equilibrium-binding parameters were determined by nonlinear least-square fitting of the quadratic form of the binding equation to data, as described before (Olson et al., 1993).

Fluorescence emission spectra

The possibility that OS changes the spectral characteristics of antithrombin was examined by comparing fluorescence spectra obtained in standard solutions to spectra in stressed solutions (3% PEG 300), with excitation at 280 nm, 4 nm bandpass, and emission bandpass at 2 nm. The presence of PEG did not induce noticeable changes in the fluorescence intensity or in the spectral tracings of the antithrombin solutions when measured either alone or in the presence of heparin at saturating concentration. The expected increases in fluorescence intensity induced by heparin were present and of indistinguishable magnitude, in tracings obtained under standard or OS conditions (data not shown).

Determination of the OS effect on the association and dissociation rates

The effect of OS on the rate of antithrombin/heparin complex formation and heparin dissociation from the ternary complex was measured in a stopped-flow fluorometer (DX. 18MV, Applied Photophysics, Leatherhead, UK) with an excitation wavelength of 280 nm, excitation slit width at 1 nm, corresponding to a bandpass of 4.65 nm, and emission filter cutoff at 320 nm. The rate of complex formation was measured by the rate of increase in intrinsic antithrombin fluorescence upon mixing with heparin. The rate of heparin dissociation from ternary complex was determined by measuring the rate of fluorescence decrease upon mixing the preequilibrated antithrombin/heparin with fXa. (In mixed solutions, the fluorescence of antithrombin and factor Xa were additive in the presence or absence of PEG 300). The rate of fluorescence increase/decrease was measured at OS levels ranging from 0 to 9 atm. In these stopped-flow kinetic measurements, osmotic stress was induced with PEG 300 at 25°C in TRIS buffer, pH 7.2–7.4, and with 0.2N NaCl. Single exponential rate coefficients were determined from the progression curves of 10 to 14 different mixings.

To determine whether OS effects were dependent on the reactants' concentrations and reaction order, measurements were repeated at increasing concentrations of one component, while maintaining the relative concentration of the remaining components. For the association reaction, antithrombin was maintained at 100 nM, while heparin was increased from 0.075 to 29 nM. For the dissociation of heparin from the ternary complex, fXa was maintained at 120 nM, while antithrombin was increased from 60 to 1886 nM, with heparin concentration maintained at a threefold molar excess over antithrombin concentration.

Miscellaneous

Equilibrium-binding parameters were derived from the dependence of fluorescence increase, ΔF_o, on the concentration of heparin. Computer fitting of the quadratic form of the binding equation to the data was used to calculate the Kh and F_{max} (maximal fluorescence change), using the program TableCurve (SAS Institute, Inc., Cary, NC). Linear regression analyses were performed with the computer program Stat-View (SAS Institute, Inc.). All results were confirmed in at least three independent sets of experiments. Antithrombin was purchased from Enzyme Laboratories (South Bend, IN) and heparin, either 8000 or 17,000 molecular weight, from Sigma (St. Louis, MO). Osmotic probes, either PEG 300 or PEG 600 and the TRIS buffer were from Fisher Scientific (Pittsburgh, PA).The pH of buffer solutions containing PEG at the concentrations used in these studies was not significantly different from the pH of solutions without PEG. The osmotic pressure of PEG solutions was calculated from previously published equations relating PEG concentrations to osmotic pressure in aqueous solutions (Parsegian et al., 1986).

Calculation of hydration volumes in antithrombin structures

Water-permeable spaces excluded by the osmotic probes in antithrombin were measured in x-ray-derived models by computational geometry using the α-shape-based software, CAST (Liang et al., 1998). The rationale and theoretical basis for this software have been described (Liang et al., 1998). Briefly, the specificity of molecular interactions are determined by the shapes of the interacting molecular surfaces. Considered at resolutions relevant to chemical reaction, the surface shapes of proteins are extremely complex with many concavities and protrusions. The surface defines distinct pockets with "mouths," or openings, connecting the inside of the concavity with bulk solvent spaces. These pockets can be considered structural units providing both shape complementarity and a specific physicochemical environment. The CAST program incorporates recent advances in computational geometry that have made possible analytical evaluation of the complex shapes of protein surfaces. This software locates and computes all pockets in proteins and calculates the metric characteristics of both the pocket and the area of the mouth(s) connecting the interior with bulk solvent spaces. The program also identifies cavities (or pockets without mouths) inside the crystal-derived protein structures. The location of pockets, their atomic composition, their volume, and the area of the mouth connecting the pocket to bulk solution constitute a unique hydration fingerprint for each protein's structure.

Hydration fingerprints of antithrombin conformers were calculated from x-ray-derived atomic coordinates in the Brookhaven Protein Data Bank files 2ant, 1azx, and 1br8. The general characteristics of these structures and their putative functional significance have been considered before (Skinner et al., 1997, 1998; Jin et al., 1997). The 2ant file includes atomic coordinates of antithrombin in an L (latent) and I (inhibitory) conformation in the absence of ligand. In the L conformer, the reactive loop is fully inserted as strand 4 of β-sheet A, whereas in the I conformer, the reactive loop is inserted from residues P10 to P14 (the nomenclature of the reactive center loop follows Schechter and Berger, 1967). The partially inserted loop separates strands 5 and 3. The 1azx file includes the coordinates of the same two conformers bound to an oversulfated heparin analog, pentasaccharide. In this structure, the P10 through P14 residues of the I conformer are not inserted, and strands 3 and 5 are closer than in the inserted conformer. The 1br8 file includes coordinates of an L conformer and an I conformer bound to a synthetic peptide with the same sequence as the reactive loop from P14 to P3. The peptide is completely inserted, forming the fourth strand of β-sheet A, similar to the L conformer of 2ant but with the reactive loop completely exposed, as in the I conformer of 1azx.

The water-permeable pockets stressed by PEG 300 were defined as pockets with mouth areas $< \pi$ (4 Å)^2. The section of PEG 300 was modeled from a sphere of 4 Å radius. This value is an average of several similar values available in the literature (Kuga, 1981; Atha and Ingham, 1981; Knoll and Hermans, 1983; Arakawa and Timasheff, 1985). For CAST calculations, the structures were prepared by separating the I and L conformers and removing ligands manually. Pocket structures corresponding to the heparin-binding region were defined as those containing atoms from residues previously demonstrated to be important in heparin binding by mutational analyses (Ersdal-Badju et al., 1998). Residues used in the search were Lys-11, Arg-13, Arg-24, Arg-47, Lys-125, Arg-129, Arg-132, and Arg-145. To analyze the shape of the reactive-loop insertion region, pockets were measured in the 1br8 I conformer after removal of the inserted peptide.

RESULTS

Equilibrium binding-parameters under osmotic stress

Water-transfer reactions during antithrombin activation by heparin were initially investigated by comparing equilibri-

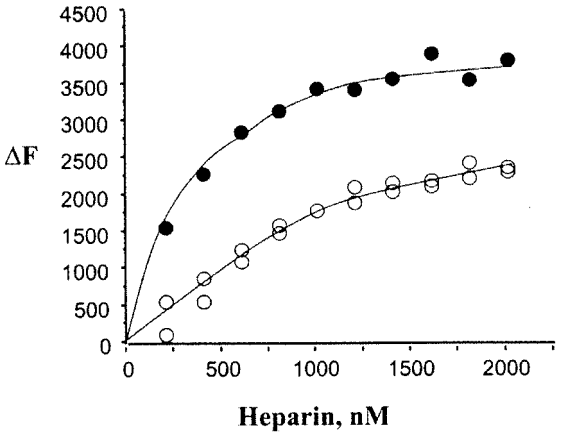

FIGURE 1 Fluorescence titration under equilibrium conditions. Heparin was equilibrated at a range of 200 to 2000 nM concentrations with antithrombin maintained at a fixed concentration of 200 nM. At each heparin concentration, the fraction of antithrombin bound was determined from the increase in its intrinsic fluorescence. ΔF is the increase in antithrombin protein fluorescence (λ_{ex} 280 nm, λ_{em} 340 nm) relative to baseline fluorescence without heparin. Standard solutions (○) were buffered with TRIS at pH 7.2 to 7.4 and contained 0.2 N NaCl. Stressed solutions (●) were identical but included PEG 300 as an OS probe at a concentration of 5% wt. Determined by fitting the quadratic form of the binding equation to data, the dissociation constant was 935 ± 156 nM in control and 236 ± 32 nM in stressed solutions, respectively. (In the figure the curves are drawn manually.)

um-dissociation constants determined under OS and standard conditions.

Equilibrium-dissociation constants were determined from titrations of antithrombin with heparin using the increase in antithrombin's intrinsic fluorescence to measure the fraction bound. In these fluorescence titration experiments, antithrombin concentration was fixed at 200 nM, whereas heparin was increased by successive additions of 200 nM each. The intrinsic fluorescence increased with heparin concentration approaching asymptotically to a maximum under both control and OS conditions (Fig. 1). The dissociation constant, calculated from fitting the quadratic form of the binding equation to data points obtained at various osmotic stress levels, was inversely correlated with the osmotic pressure. In solutions with PEG 300 (~4 Å radius), the slope $\Delta(\Delta G)/\Delta\pi$ was -103 ± 38 and -165 ± 42 cal/mol/atm at NaCl concentrations of 0.075 and 0.2 N, respectively. These slope values correspond to 237 ± 87 and 379 ± 96 water molecules, respectively. The magnitude of the OS effect appeared to be correlated with the size of the probe. In experiments with PEG 600 (7 Å radius) at 0.075 N NaCl, the slope value was -286 ± 71 cal/mol/atm, corresponding to 657 ± 163 molecules of water. The typically large errors involved in determining dissociation constants by equilibrium fluorescence titrations, preclude more precise determination of the magnitude of transferred volumes and the salt concentration effect. However, in functional titration experiments, osmotic effects on biding parameters were very dependent on salt concentrations.

Maximal enhancement of antithrombin fluorescence intensity was $43 \pm 5\%$ and $43 \pm 4\%$ in PEG 300 and PEG 600 solutions, respectively, and similar to that in standard solutions: $44 \pm 4\%$.

The decrease in the dissociation constant for the heparin/antithrombin interaction under osmotic stress indicates that the equilibrium position shifted toward complex formation. This result is consistent with net water transfer from reactants to bulk on formation of the complex.

Effect of OS on association and dissociation rates measured in the stopped-flow fluorometer

The results from equilibrium experiments indicated that the complex is dehydrated relative to reactants in solution. To further analyze the interaction, we measured the effect of OS on the association and dissociation rates in a stopped-flow fluorometer under pseudo-first-order conditions. In these experiments, OS was induced with PEG 300 at pH 7.2 and 0.2 N NaCl. Association rates were measured from the increase in fluorescence on mixing antithrombin and heparin. Dissociation rates were determined from the decrease in the fluorescence of antithrombin, equilibrated with excess heparin, upon addition of fXa. Fig. 2, *A* and *B* show representative tracings of k_{obs} for association and dissociation reactions under either control or OS conditions.

Association reaction

To determine the order of the association reaction, rates were measured at a range of heparin concentrations, while maintaining the antithrombin concentration constant. The rate increased linearly with heparin concentration up to 15 μM, giving second-order rate constants of 5.2 ± 0.2 and 4.0 ± 0.1 μM^{-1} s^{-1} with and without OS. The k_{off} determined from the ordinate intercept in plots of rate versus heparin concentration was 1.3 s^{-1} in control solutions and not significantly different from 1.1 s^{-1} in stressed solutions (Fig. 3 *A*).

The rate of antithrombin-heparin complex formation was then measured at fixed concentrations of heparin (15 μM) and antithrombin (100 nM), while varying OS levels from 0 to 6 atm. The association rate increased with OS. The $\Delta(\Delta G‡)/\Delta\pi$ slope was -66.9 ± 4.2, corresponding to 158 ± 11 waters transferred from reactants to bulk during the rate-determining step of the fluorescence-enhancement transition (Fig. 4 *A*).

Dissociation reaction

The rate of dissociation of heparin from the ternary complex was measured by following the reversal of the fluorescence

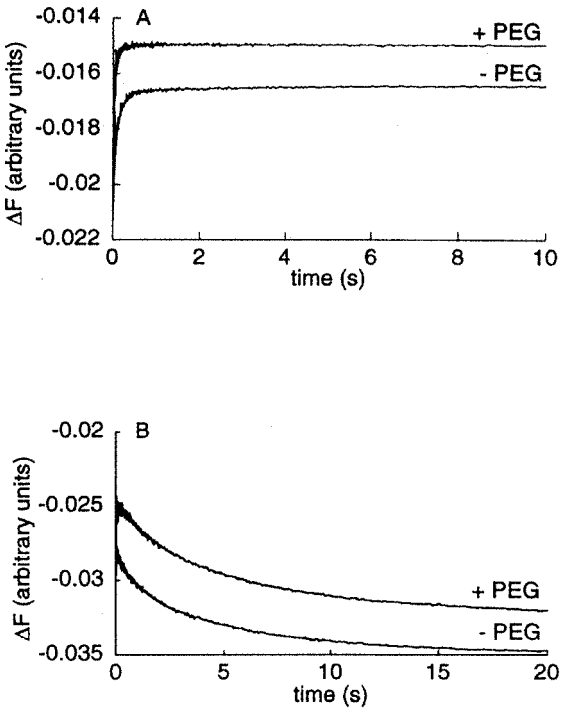

FIGURE 2 Rapid kinetics of antithrombin fluorescence enhancement/decrease on heparin binding/release. Reaction rates were followed in the stopped-flow fluorometer at room temperature in TRIS buffer pH 7.2 to 7.4 and 0.2 N NaCl. Osmotic stress was induced with PEG 300 at 5% weight/volume. (*A*) Tracings of the rate of intrinsic antithrombin (100 nM) fluorescence enhancement upon mixing with heparin (15 μM) under either standard (−PEG) or osmotic stress conditions (+PEG). (*B*) Tracings of the rate of fluorescence decrease on mixing antithrombin (100 nM preequilibrated with 300 nM heparin) with fXa (120 nM) under either standard (−PEG) or osmotic stress conditions (+PEG).

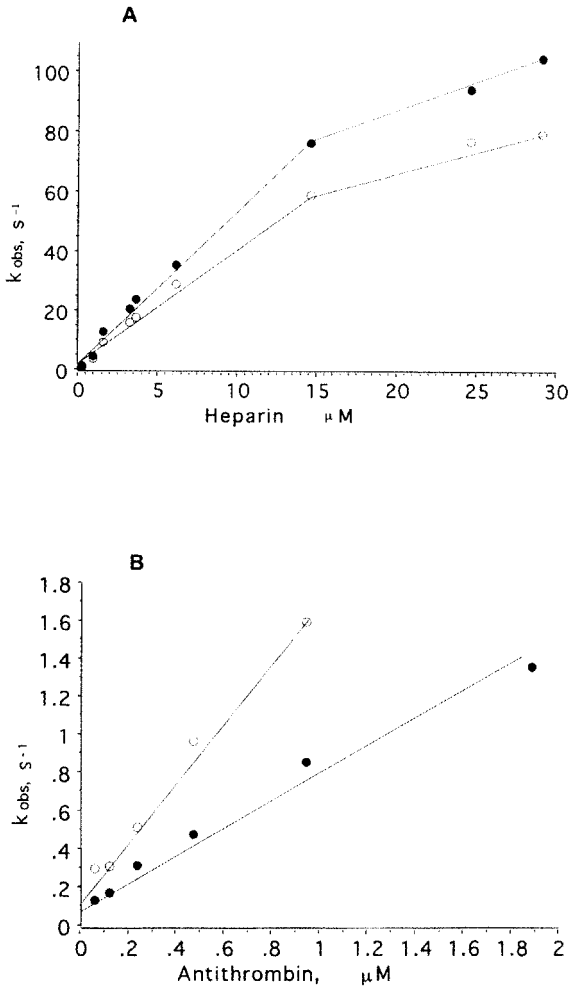

FIGURE 3 Concentration dependence of reaction rates. Rates were measured at the range of concentrations indicated in the abscissa in the stopped-flow fluorometer. Other conditions were as indicated in the legend to Fig. 2. Each point is an average of 10 to 14 rate measurements. (*A*) Rate of antithrombin fluorescence enhancement at different heparin concentrations under standard (○) and OS conditions (●). (*B*) Rate of fluorescence decrease at different antithrombin/heparin concentrations under standard (○) and OS conditions (●).

enhancement reaction upon mixing preequilibrated antithrombin/heparin solutions with fXa. In contrast to the effect of OS on the rate of fluorescence enhancement, OS decreased the rate of fluorescence reversal. The initial slopes k_{obs} versus antithrombin concentration were 0.81 ± 0.03 and 1.5 ± 0.07 μM^{-1} s^{-1} in stressed and standard solutions, respectively. The ordinate intercepts were 0.183 and 0.096 s^{-1} in stressed and standard solution, respectively, for antithrombin concentrations ranging from 0.06 to 1.8 μM (Fig. 3 *B*).

The change in the dissociation rate with OS was determined at pressures ranging from 0 to 9 atm and at fixed antithrombin (100 nM), heparin (300 nM), and fXa (120 nM) concentrations. In contrast to the association reaction, the slope was positive, with a value of 73.26 ± 9.6 cal/mol/atm corresponding to 168 ± 22 waters (Fig. 4 *B*). Results show that upon formation of the ternary complex, the dissociation of heparin is subjected to an unfavorable osmotic potential and, consequently, linked to water transfer from bulk to reactants.

Comparison between water transfer measurements from equilibrium and kinetic experiments

The number of water molecules transfer measured at equilibrium, $\Delta N_{w,\,eq.}$, was compared with volumes measured during the association, $\Delta N_{w,\,ass.}$, and dissociation, $\Delta N_{w,diss}$, reactions.

Assuming that hydration changes during the dissociation of heparin from the ternary complex are not different from changes during its dissociation from the binary complex, the expected relationship between the volumes determined in equilibrium and kinetic measurements is,

$d(\ln Kh)/d\pi = d(\ln k_{diss})/d\pi - d(\ln k_{ass})/d\pi$ or the equivalent, $\Delta N_{w,\,eq} = \Delta N_{w,\,diss} - \Delta N_{w,\,ass}$.

Thus, using the volumes determined from the effect of OS in reaction rates, the calculated value of $\Delta N_{w,\,eq}$, is,

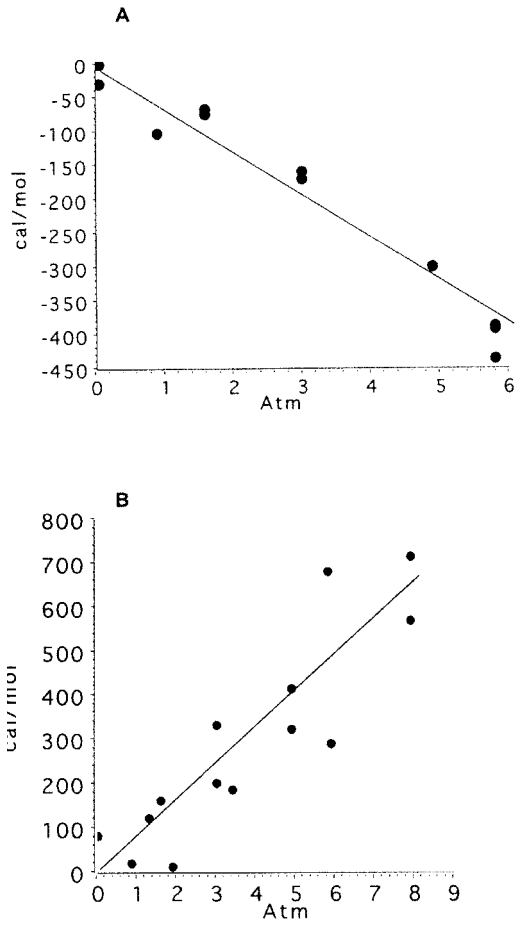

FIGURE 4 Change in the free energy of activation with OS for association and dissociation of antithrombin from heparin. Reaction rates were measured at the range of osmotic stress indicated in the abscissa. Other conditions were as indicated in the legend to Fig. 2. Free energy of activation, $\Delta G\ddagger$, was calculated from the rate coefficient according to "rate reaction theory" and classical thermodynamic principles (Glasstone et al., 1941). Data are from three sets of independent experiments; each $\Delta G/\pi$ data point is the mean of at least 10 rate measurements. (*A*) Change in the free energy of activation for association reactions. The slope value was -158 ± 11 cal/mol/atm. (*B*) Change in the free energy of activation for dissociation reactions. The slope value was 162 ± 22 cal/mol/atm.

$162 - (-158) = 320$. This value is similar to the value 379 ± 96 determined in equilibrium titration experiments from the effect of OS in the dissociation constant.

Water-permeable spaces in x-ray-derived antithrombin structures

Previous structure/function studies (Huntington et al., 1996; Beauchamp et al., 1998) support the idea of a link between occupation of the cationic groove of antithrombin by heparin and expulsion of the reactive loop from β-sheet A. Because we find that heparin binding/release is also linked to water transfer, antithrombin structures corresponding to free and bound conformations should have different hydration volumes. To gain further insight into the functional significance of available structures, we measured the volume of their water-permeable pockets using analytical computational geometry.

Loop-insertion pocket

The hydration volume of the loop-insertion region was measured in PDB data file 1br8 I. In this conformer, the reactive loop is completely expelled, but in the β-sheet A, strands 3 and 5 remain separated due to presence of an inserted synthetic peptide with a sequence identical to that of the reactive loop. To model the insertion region, the peptide was removed manually and the structure with the insertion region left empty was analyzed using the software CAST (Liang et al., 1998). Results reveal that the insertion region is a large continuous tubular pocket with a volume of 1941 $Å^3$ (~65 water molecules) and accessible to bulk water via five different openings. (Fig. 5 *A*). This pocket does not exist in the 1azx structures and only in a rudimentary form in the 2ant I structure.

Heparin-binding region

The hydration volumes in the heparin-binding region was analyzed in PDB data file 1azx I, representing an activated antithrombin conformer. In this model, the heparin groove is partially occupied by an oversulfated pentasaccharide analog. This ligand was removed manually before measuring the water-permeable volumes using CAST. Water accessible volumes in the heparin-binding region were identified as pockets containing atoms from residues Lys-11, Arg-13, Arg-24, Arg-47, Lys-125, Arg-129, Arg-132, Arg-145, previously implicated in heparin binding by mutational analyses (Ersdal-Badju et al., 1998). Results indicate that the surface of the heparin-binding region in 1azx I includes 8 distinct pockets with a total volume of 1523 $Å^3$ (~50 water molecules). The heparin-binding region was also measured in the free antithrombin conformer 2ant I. In this conformer, the heparin-binding residues were also in eight different pockets, but their combined hydration volume was 724 $Å^3$ (~24 water molecules). The difference between the volume of the heparin-binding region in bound and free antithrombin corresponds to 26 water molecules.

Shared residues

Analyses of the atomic composition of the loop-insertion and heparin-binding regions indicated that several amino acid residues contribute atoms to both. Residues contributing atoms to both the loop-insertion and heparin-binding pockets are Ala-86, Val-214, Leu-215, Asn-217, Ser-79, Ile-219, and Thr-218. Interestingly, many of the atoms shared by the loop-insertion and heparin-binding pockets

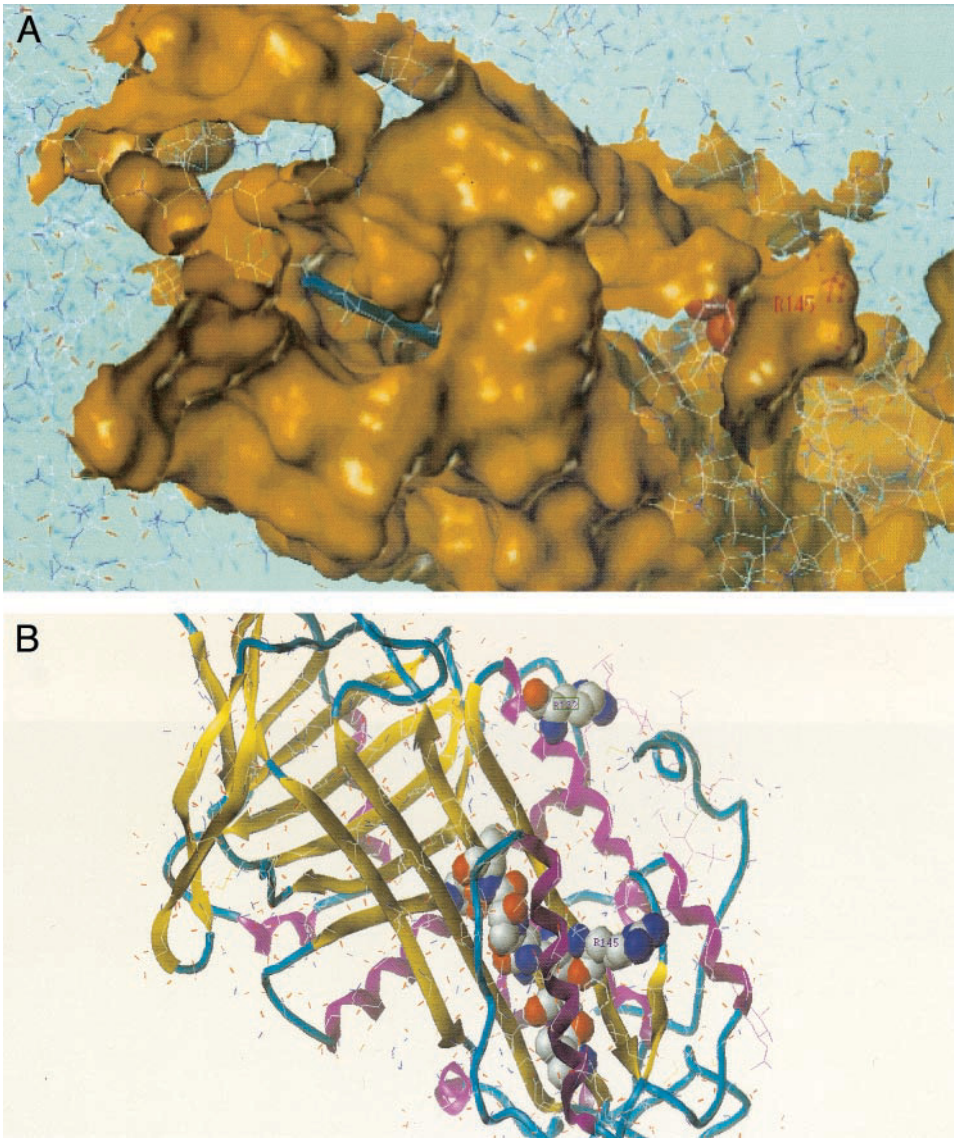

FIGURE 5 The water-permeable spaces in loop-insertion regions and residues shared with heparin-binding regions. (*A*) The surface of the loop-insertion pocket in 1br8. The surface was calculated after removing a fully inserted peptide corresponding to residues P14 to P3 of the reactive loop. Surfaces were calculated by the Connolly method implemented with MOLCAD. The figure represents water-accessible surface (in *dark orange*), excluding the peptide surface, within 8 Å from the peptide. The peptide (rendered in *blue*) is buried and visible only at one of the pocket's openings. The rest of the antithrombin structure is rendered as a line model of atom bonds, except for residue R 145, which is rendered as a space-filling model (*red*). (*B*) The residues contributing atoms to both the heparin and the loop-insertion region are represented as space-filling spheres over a ribbon/tube rendition of the antithrombin structure 1azx, conformer I. Note how most of the shared residues are strategically distributed along strand 3 of β-sheet A. The residues and shared atoms are listed in Table 1.

are β carbons. The distribution of residues is shown in Fig. 5 *B*, and the atoms are listed in Table 1.

Pocket location of tryptophan residues

The environment of tryptophan residues relative to pocket-structures was also investigated. All four residues, Trp-49, Trp-189, Trp-225, and Trp-307, contribute atoms to well-defined pocket structures in both heparin-bound, 1azx, and free 2ant antithrombin conformers. None of the four residues except Trp-189 contribute atoms to heparin-binding pockets. In addition, Trp-225 in 1azx I and 2ant I is in a pocket cavity with no opening, but in the 1br8 I conformer it is next to the loop-insertion pocket and exposed to solvent. This observation suggests that the opening and closing of strands 4 and 3 of β-sheet A, during heparin-induced expulsion and reinsertion transitions, drastically change this residue's environment.

The total volume of Trp-containing pockets in the bound, loop-exposed conformer 1azx I is 2296 Å^3 and larger than the volume of 1042 Å^3 measured for Trp-containing pockets in the free conformer 2ant I. The total area of the openings, or mouths, of Trp-containing pockets in the bound, loop-exposed conformer 1azx I was 296 Å^2 and larger than the area 127 Å^2 measured in the free, 2ant I conformer. The volumes in Trp-containing pockets found in the loop inserted conformers were 868 and 798 Å^3 for the bound 1azx L and free 2ant L conformer, respectively. The corresponding areas of the pocket openings were 230 and 156 Å^2 in 1azx L and 2ant L, respectively. Considering only Trp-225 and Trp-307, however, the volume of the pockets is 490 and 601 Å^3 in 1azx I and 2ant I, respectively, suggesting that

TABLE 1 Residues that contribute atoms to pockets in the heparin and loop-insertion regions

	Atoms lining pockets	
Shared Residues	Heparin-binding	Loop-insertion
Ala-86	CB	O, C, CB
Val-214	O, C, N	CA, CG1, CG2
Leu-215	CG, CB	N, O, CB, CD1, CD2
Asn-217	ND2	N, O, CB
Ser-79	CB	CB
Ile-219	CD1, CB	N, O, CB
Thr-218	O, N	CG2
Asn-217	CB, C	N, O, CB

This table includes the residues and atoms from heparin-binding pockets in 1azx that were also found in the peptide pocket of 1rb8 I. Pockets in 1azx I that contain atoms from residues implicated in heparin binding were selected (Ersdal-Badju et al., 1998). Pockets were identified using the α-shaped-based software CAST. The heparin-binding pockets in 1azx I contained atoms from R145 and R132. The structures were prepared manually by removing the ligands, a pentasaccharide analog in 1azx I, and a peptide with the same amino acid sequence as the reactive center loop in 1rb8 I. Individual atoms shared by the heparin-binding and loop-insertion pockets are underlined. Atoms' nomenclature follows PDB file convention.

these residues are closer to neighboring groups and that their environment is more dehydrated in the antithrombin/heparin complex than in free antithrombin. These two Trp residues have been shown to contribute ~75% of the total fluorescence changes induced by heparin binding/release. (Olson and Shore, 1981; Meagher et al., 1998).

DISCUSSION

In these studies, osmotic stress was applied to analyze hydration changes in antithrombin during conformational transitions induced by heparin. In the presence of osmotic probes excluded from antithrombin's water-permeable spaces, the equilibrium of the antithrombin/heparin interaction shifted toward complex formation. The free energy of the binding interaction measured under equilibrium conditions decreased as the osmotic pressure of bulk solution increased. Results from association and dissociation rate measurements using stopped-flow methods indicated that, within experimental error, the hydration volumes transferred to bulk during heparin binding are of the same magnitude as the volumes transferred back to the reactants during dissociation. Osmotic stress accelerated the rate of fluorescence increase, and from the decrease in the free energy of activation with pressure, we calculated the transfer of 158 ± 11 water molecules during the association reaction. In contrast, OS decreased the rate of antithrombin fluorescence decay during heparin release from the ternary complex. From the increase in free energy of activation with osmotic pressure, we calculated the transfer of 162 ± 22 molecules of water from bulk to reactants during the dissociation.

The volume transfer determined in equilibrium experiment is consistent with the volume calculated from the kinetic measurement of the heparin association and dissociation reactions. Because the protease is present during heparin dissociation, this observation supports the idea that the proteinase does not have a major impact in the hydration of the antithrombin-heparin complex. Previous mutational studies of thrombin, another target proteinase of antithrombin, also indicated that, aside from the active/reactive site interactions, there are no close contacts between the antithrombin and proteinase surfaces in the complex (Tsiang et al., 1997).

Analytical computation of water-permeable volumes in x-ray-derived models were also consistent with water transfer during both the association and dissociation reactions. Conformational changes are evident at the loop-insertion region and the heparin-binding site (Jin et al., 1997). Our geometrical computations further indicate that the heparin-binding and loop-insertion regions could contribute ~90 molecules of water. This volume is significantly less than transfer volumes measured during association and dissociation reactions. An exact quantitative correspondence between the hydration spaces in the x-ray-derived model structures and the measured transfer volumes in solution was not expected. Although the computational calculations of volume are analytical, the crystal-based structures may not correspond to the reacting ensemble's mean conformation. Available antithrombin crystals are generated under osmotic stress conditions, and it is unlikely that the volumes of the superficial pockets in either the heparin-binding or loop-insertion regions coincide with their volume in diluted solution. The discrepancy may be particularly large outside the regions occupied by the pentasaccharide analog in 1azx I and in the region immediately underlying the partially inserted reactive loop in 2ant I. The length of the heparin and the extent of loop insertion are likely to influence the pockets' volume during the reaction. The volume of the loop-insertion region in the 1br8 I structure may be closer to the actual volumes transferred. This volume was measured using the cast left by the P14-P3 peptide in β-sheet A and represents the volume that must be displaced to achieve full insertion of the reactive-site loop. It is also tempting to speculate that some of the water transfer could derive from the surface hydration of heparin. In solution, heparin is expected to remain extended rather than coiled due to the high density of negative charges (Parthasarathy et al., 1994). Assuming complete occupation of a 50 Å-long binding groove (Ersdal-Badju, 1997), the volume excluded by PEG 300 in the corresponding docking surface of heparin, estimated using the excluded volume theory approximation (Hermans, 1982), would be ~ 1256 Å^3. This volume corresponds to ~42 molecules of water and would bring the calculated volumes within the range of transfer volumes measured by OS. Despite the approximations involved and the possibility that some volumes are not accounted for in

the computations, the large differences in hydration volumes measured at the loop and heparin-binding regions strongly suggest that at least part of the measured water transfer in solution is from these regions.

The water transfer measured by OS during macromolecular interactions does not necessarily correspond to the volume changes measured using hydrostatic pressure (Low and Somero, 1975). The osmotic stress technique measures changes in the number of waters, whereas hydrostatic pressure studies measure volume changes resulting from both hydration density and conformation changes. In the OS calculations, the possible effects on water structure of exposed protein groups are ignored, and the density of water in the excluded volumes is assumed to be the same as in bulk solution. This assumption is justified by results from nuclear magnetic resonance evaluations, indicating that the velocity of the molecular motions of surface water is close to that of bulk water (Bryant, 1996). These nuclear magnetic resonance results do not exclude the possibility that very short-lived "structured water" may contribute to the volume differences measured during reactions.

Together with previously published studies, the osmotic stress and computational analyses presented here further suggest that the conformational transitions induced by heparin are structurally linked to changes in the hydration volumes of antithrombin. Globally, the water-transfer reactions during antithrombin activation can be summarized as a three-step sequence. In the first conformational transition, water is transferred from the heparin-binding and loop-insertion regions to bulk solution, coinciding with heparin docking and loop release. The second transition follows the initial binding of fXa and formation of the ternary complex. This interaction releases heparin and reopens the β-sheet A strands, forming water-permeable pockets at the loop and heparin pockets. Simultaneously, water is transferred from bulk to refill these pockets. Finally, the reactive loop is reinserted, and the protease is dragged along, narrowing the large interprotein spaces formed during the initial reversible interaction (Futamura and Gettins, 2000). Water is again released, now irreversibly, from the loop-insertion region and from the interprotein spaces (Liang and McGee, 1998).

Results from analyses of the atomic composition of the water-permeable pockets suggest a structural explanation for the propagation of heparin binding/release signals to the loop-insertion region. The surface of pockets in the heparin-binding region is formed, in part, by atoms from residues of strand 3 of β-sheet A in the loop-insertion region. In fact, the β-carbons of Ser-79, Ala-86, Leu-215, Asn-217, and Ile-219 are part of the water-accessible surface in both the heparin-binding region and the loop-insertion region. Previous observations in two familiar and one experimental mutations (Beauchamp et al., 1998; Lee et al., 1998) also implicate the loop insertion-region modulating the serpins stability and heparin affinity. The presence of common residues in the wall of water-accessible pockets in the loop-insertion and heparin-binding regions suggests a mechanism that helps to explain the heparin-induced conformational changes of antithrombin. Even subtle changes in the position of common residues would be transmitted through the β-carbons across the pocket's wall to the loop-insertion region during heparin binding/release. Similarly, changes in common residues during loop insertion would be transmitted to the heparin-binding surface. Considering the water-accessible pockets as structural units, the activation signal mediated by heparin docking involves a direct transmission across common sites in the pockets' wall, rather than the more indirect allosteric effect suggested by measurement of distances across peripheral atoms.

This work was supported by NSF grant MCB-9601411 and National Institutes of Health-HL 57936. The computational geometry component was supported in part by NSF grant DBI-0078270 to J. Liang.

REFERENCES

Arakawa, T., and S. N. Timasheff. 1985. Mechanisms of poly(ethylene glycol) interaction with proteins. *Biochemistry.* 24:6756–6762.

Atha, D. H., and K. C. Ingham. 1981. Mechanism of precipitation of proteins by polyethylene glycols: analysis in term of excluded volume. *J. Biol. Chem.* 256:12108–12117.

Beauchamp, N. J., R. N. Pike, M. Daly, L. Butler, M. Makris, T. R. Dafforn, A. Zhou, H. L. Fitton, F. E. Preston, I. R. Peake, and R. W. Carrell. 1998. Antithrombins Wibble and Wobble (T85M/K): archetypal conformational diseases with in vivo latent-transition, thrombosis, and heparin activation. *Blood.* 92:2696–2706.

Bryant, R. G. 1996. The dynamics of water-protein interactions. Annu. Rev. Biophys. Biomol. Struct. 25:29–53.

Carrell, R. W., D. L. Evans, and P. E. Stein. 1991. Mobile reactive centre of serpins and the control of thrombosis. *Nature.* 353:576–579.

Colombo, M. F., D. C. Rau, and V. A. Parsegian. 1992. Protein solvation in allosteric regulation: a water effect on hemoglobin. *Science.* 256: 655–659.

Connolly, M. L. 1983. Analytical molecular surface calculations. *J. Appl. Cryst.* 16:548–558.

Craig, P. A., S. T. Olson, and J. D. Shore. 1989. Transient kinetics of heparin-catalyzed protease inactivation by antithrombin III: characterization of assembly, product formation, and heparin dissociation steps in the factor Xa reaction. *J. Biol. Chem.* 264:5452–5461.

Desai, U. R., M. Petitou, I. Bjork, and S. T. Olson. 1998. Mechanism of heparin activation of antithrombin: evidence for an induced-fit model of allosteric activation involving two interaction subsites. *Biochemistry.* 37:13033–13041.

Douzou, P. 1994. Osmotic regulation of gene action. *Proc. Natl. Acad. Sci. U.S.A.* 91:1657–1661.

Ersdal-Badju, E., A. Lu, Y. Zuo, V. Picard, and S. C. Bock. 1997. Identification of the antithrombin III heparin binding site. *J. Biol. Chem.* 272:19393–19400.

Futamura, A., and P. G. Gettins. 2000. Serine 380 (P14) → glutamate mutation activates antithrombin as an inhibitor of factor Xa. *J. Biol. Chem.* 275:4092–4098.

Glasstone, S., K. Laidler, and H. Eyrin. 1941. The Theory of Rate Processes. McGraw-Hill, New York. 1–27.

Hermans, J. 1982. Excluded-volume theory of polymer-protein interactions based on polymer chain statistics. *J. Chem. Phys.* 77:2193–2203.

Hochachka, P. W., and G. N. Somero. 1973. Strategies of Biochemical Adaptation. W. B. Saunder Co., Philadelphia. 358.

Huntington, J. A., S. T. Olson, B. Fan, and P. G. Gettins. 1996. Mechanism of heparin activation of antithrombin: evidence for reactive loop prein-

sertion with expulsion upon heparin binding. *Biochemistry.* 35: 8495–8503.

Jin, L., J. P. Abrahams, R. Skinner, M. Petitou, R. N. Pike, and R. W. Carrell. 1997. The anticoagulant activation of antithrombin by heparin. *Proc. Natl. Acad. Sci. U.S.A.* 94:14683–14688.

Johnson, F. H., and H. Eyrin. 1970. High Pressure Effects on Cellular Processes. A. H. Zimmerman, editor. Academic Press, New York. 1–44.

Jordan, R. E., G. M. Oosta, W. T. Gardner, and R. D. Rosenberg. 1980. The kinetics of hemostatic enzyme-antithrombin interactions in the presence of low molecular weight heparin. *J. Biol. Chem.* 255:10081–10900.

Knoll, D., and J. Hermans. 1983. Polymer-protein interactions: comparison of experiment and excluded volume theory. *J. Biol. Chem.* 258: 5710–5715.

Kuga, S. 206. 1981. Pore size distribution analysis of gel substances by size exclusion chromatography. *J. Chromat.* 206:449–461.

Kvassman, J. O., I. Verhamme, and J. D. Shore. 1998. Inhibitory mechanisms of serpins: loop insertion forces acylation of plasminogen activator by plasminogen activator inhibitor 1. *Biochemistry.* 37: 15491–15502.

Lane, D. A., R. R. Olds, and S. L. Thein. 1992. Antithrombin and its deficiency states. *Blood Coagul. Fibrinolysis.* 3:315–341.

Lawrence, D. A. 1997. The serpin-proteinase complex revealed. *Nat. Struct. Biol.* 4:339–341.

Lee, K. N., H. Im, S. W. Kang, and M.-H. Yu. 1998. Characterization of a human α 1-antitrypsin variant that is as stable as ovalbumin. *J. Biol. Chem.* 273:2509–2516.

Liang, J., H. Edelsbrunner, P. Fu, P. V. Sudhakar, and S. Subramanian. 1998. Analytical shape computation of macromolecules: I. Molecular area and volume through alpha shape. *Proteins.* 33:1–17.

Liang, J., H. Edelsbrunner, and C. Woodward. 1998. Anatomy of protein pockets and cavities: measurement of binding site geometry and implications for ligand design. *Protein Sci.* 7:1884–1897.

Liang, J., and M. P. McGee. 1998. Hydration structure of antithrombin conformers and water transfer during reactive loop insertion. *Biophys. J.* 75:573–582.

Low, P. S., and. G. N. Somero. 1975. Protein hydration changes during catalysis: a new mechanism of enzymic rate-enhancement and ion activation/inhibition of catalysis. *Proc. Natl. Acad. Sci. U.S.A.* 72: 3305–3309.

Meagher, J. L., J. M. Beechem, S. T. Olson, and P. G. Gettins. 1998. Deconvolution of the fluorescence emission spectrum of human antithrombin and identification of the tryptophan residues that are responsive to heparin binding. *J. Biol. Chem.* 273:23283–23289.

Olson, S. T., I. Bjork, and J. D. Shore. 1993. Kinetic characterization of heparin-catalyzed and uncatalyzed inhibition of blood coagulation proteinases by antithrombin. *Methods Enzymol.* 222:525–559.

Olson S. T., and J. D. Shore. 1981. Binding of high affinity heparin to antithrombin III. Characterization of the protein fluorescence enhancement. *J. Biol. Chem.* 256:11065–11072.

Parsegian, V. A., R. P. Rand, N. L. Fuller, and D. C. Rau. 1986. Osmotic stress for the direct measurement of intermolecular forces. *Methods Enzymol.* 227:400–416.

Parsegian, V. A., R. P. Rand, and D. C. Rau. 2000. Osmotic stress, crowding, preferential hydration, and binding: a comparison of perspectives. *Proc. Natl. Acad. Sci. U. S. A.* 97:3987–3992.

Parthasarathy, N., I. J. Goldberg, P. Silvaram, B. Mulloy, D. M. Frory, and W. D. Wagner. 1994. Oligosaccharide sequences of endothelial cell surface heparan sulfate proteoglycan with affinity for lipoprotein lipase *J. Biol. Chem.* 269:22391–22396.

Rand, R. P. 1992. Raising water to new heights. *Science.* 256:618.

Sakabe, N., K. Sakabe, and K. Sasaki. 1981. Structural Studies of Molecules of Biological Interest. G. Dodson, J. P. Glusker, and D. Sayre, editors. Clarendon, Oxford. 509–526.

Schechter, I., and A. Berger. 1967. On the size of active sites in proteases. *I. Papain. Biochem. Biophys. Res. Commun.* 27:157–162.

Skinner, R., J. P. Abrahams, J. C. Whisstock, A. M. Lesk, R. W. Carrell, and M. R. Wardell. 1997. The 2.6 Å structure of antithrombin indicates a conformational change at the heparin binding site. *J. Mol. Biol.* 266:601–609.

Skinner, R., W. S. Chang, L. Jin, X. Pei, J. A. Huntington, J. P. Abrahams, R. W. Carrell, and D. A. Lomas. 1998. Implications for function and therapy of a 2.9 Å structure of binary-complexed antithrombin. *J. Mol. Biol.* 283:9–14.

Schreuder, H. A., B. deBoer, R. Dijkema, J. Mulder, H. J. Theunissen, P. D., Grootenhuis, and W. G. Hol. 1994. The intact and cleaved human antithrombin III complex as a model for serpin-proteinase interaction. *Nat. Struct. Biol.* 1:48–54.

Stratikos, E., and P. G. Gettins. 1999. Formation of the covalent serpin-proteinase complex involves translocation of the proteinase by more than 70 Å and full insertion of the reactive center loop into β-sheet A. *Proc. Natl. Acad. Sci. U.S.A.* 96:4808–4813.

Tsiang, M. Jain, A. K., and C. S. Gibbs. 1997. Functional requirements for inhibition of thrombin by antithrombin III in the presence and absence of heparin. *J. Biol. Chem.* 272:12024–12029.

Wilczynska, M., M. Fa, J. Karolin, P. I. Ohlsson, L. B. Johansson, and T. Ny. 1997. Structural insights into serpin-protease complexes reveal the inhibitory mechanisms of serpins. *Nat. Struct. Biol.* 4:354–357.

Zhou, A., J. A. Huntington, and R. W. Carrell. 1999. Formation of antithrombin heterodimer in vivo and the onset of thrombosis. *Blood.* 94:3388–3396.